ELECTRON DIFFRACTION ANALYSIS OF THE M_{412} INTERMEDIATE OF BACTERIORHODOPSIN

R. M. GLAESER,* J. BALDWIN,‡ T. A. CESKA,‡ AND R. HENDERSON‡

Department of Biophysics and Medical Physics, and Donner Laboratory, Lawrence Berkeley Laboratory, University of California, Berkeley, California 94720; and ‡Medical Research Council Laboratory of Molecular Biology, Hills Road, Cambridge, CB2 2QH, United Kingdom

ABSTRACT   High resolution electron diffraction data have been recorded for glucose-embedded purple membrane specimens in which bacteriorhodopsin (bR) has been trapped by cooling slowly to below −100°C under continuous illumination. Thin films (OD ∼0.7) of glucose-embedded membranes, prepared as a control, showed virtually 100% conversion to the M state, and stacks of such thin film specimens gave very similar x-ray diffraction patterns in the bR_{568} and the M_{412} state in most experiments. To be certain that any measured differences in diffraction intensity would be real, two independent sets of electron diffraction intensities were recorded for near-equatorial, i.e. (hkO), reflections. Little correlation was indeed observed between these two sets for ΔF values at low resolution (15–5.0 Å, 49 reflections), but the correlation coefficient is ∼0.3 at high resolution (5.0–3.3 Å, 218 reflections). Thus, while most of the measured difference is error, the mean ΔF and the correlation coefficient can be used to estimate the smaller, true ΔF due to structural changes occurring in the M state. The magnitude of this estimated true mean ΔF is equal to what would be produced if approximately five to seven nonhydrogen atoms were moved to structurally uncorrelated (i.e., new) positions in the M state. Movements of a few amino acid side chains, and repositioning of atoms of the retinal group and the associated lysine side chain after *trans-cis* isomerization, are the most probable causes of the observed intensity changes in the M state. The difference Fourier map, calculated in projection at 3.5-Å resolution, shows only very small peaks, the largest of which are confined, however, to the region of the protein.

INTRODUCTION

The purple membrane of *Halobacterium halobium* (Oesterhelt and Stoeckenius, 1971) consists of a two-dimensional crystalline array of a single protein, bacteriorhodopsin (bR), which uses the energy of light absorbed by its covalently bound retinal group to pump protons (or hydroxyl ions) across the cell membrane (Oesterhelt and Stoeckenius, 1973). The photocycle of this light-driven proton pump consists of four or more distinct structural intermediates, which can be recognized from the time-resolved visible absorption spectra recorded in flash spectrophotometric measurements (Lozier and Niederberg, 1977). The structural intermediate designated M_{412} is the best characterized of these intermediates. The lifetime of the M_{412} state, ∼5–10 ms at 20°C, is much longer than that of intermediates that precede it, and specimens can be trapped indefinitely in the M state at temperatures below −60°C (Becher et al., 1978).

A wide range of spectroscopic tools have been used to identify a variety of chemical and structural changes that occur in the formation of the M_{412} intermediate. Resonance Raman spectroscopy has demonstrated that the retinal-lysine Schiff base is deprotonated in M (Lewis et al., 1974) and the retinal itself is isomerized from the all *trans* to the 13 *cis* conformation (Braiman and Mathies, 1980). Fourier transform infrared spectroscopy demonstrates the protonation of at least one carboxyl group in the protein (Rothschild et al., 1981; Siebert et al., 1982) and chemical studies indicate that a tyrosinate ion is also formed (Rosenbach et al., 1982; Fukumoto et al., 1984). Extensive changes occur in the near ultraviolet (UV) absorption spectrum, which have been interpreted to be due to the movement of several aromatic residues from a hydrophobic environment to a hydrophilic one (Becher et al., 1978). A large shift in the visible absorption spectrum itself, which moves the absorption peak from 568 to 412 nm, is also an independent indication that a significant structural change has occurred in the formation of this intermediate.

There is not yet any direct structural or stereochemical information concerning movements of specific amino acid side chains, or modifications of the tertiary structure that occur during the formation of the M intermediate. It is possible that the observed protonation and deprotonation reactions and isomerization of the retinal group could occur within a fairly rigid protein framework. The movements of aromatic side chains which were proposed on the basis of the near UV spectra might be very near to the surface of the membrane, once again making it possible that the major part of the protein structure could be quite rigid. On the other hand, it is equally possible that the structural changes detected in spectroscopic measurements represent but one facet of a much larger conformational

change that occurs in the M intermediate. Time-resolved x-ray diffraction studies of the M intermediate suggest that conformational changes occur that are large enough to disrupt partially the lattice bonding forces, as judged by the disorder introduced into the diffraction patterns of samples in the M state (Frankel and Forsyth, 1985). Other authors have also suggested, on the basis of circular dichroism spectra in the visible region (Draheim and Cassim, 1985), and on the basis of transient responses in the flash-induced linear dichroism signal (Ahl and Cone, 1984), that the crystalline packing of bR can become disordered in the M state.

Here we have found that glucose-embedded samples of purple membrane can be trapped in the M state with no apparent change in either the long-range order or the short-range order of the lattice. Although the crystalline lattice is not disordered when our specimens are prepared in the M state, we cannot rule out the possibility that initial dissociation of the original lattice contacts, followed by the formation of new crystalline bonds, occurs between molecules in the M state. The electron diffraction patterns of samples in the M state show small but statistically significant changes in intensity relative to the native, bR_{568} patterns. The diffraction data show significant changes only at high resolution, indicating that conformational changes in the M state are small. In addition, the number of nonhydrogen atoms involved in the structural changes appear to be no more than six to seven, i.e., only a few amino acid residues. The difference Fourier map calculated at 3.5-Å resolution confirms that there is not a single, large structural change involved in the formation of the M intermediate.

METHODS

Thin Film Control Samples

Thin films of glucose embedded purple membrane were prepared on very thin (10 μm) mylar to perform spectroscopic and x-ray diffraction experiments on the trapping of bR in the M_{412} state. Purple membrane, washed in distilled water, was mixed with an appropriate volume of 1% glucose (0.2% sodium azide) to yield a final suspension consisting of 0.125% bR and 0.5% glucose. Three drops of the suspension of purple membrane in 0.5% glucose were put onto individual pieces of mylar film, mounted on glass coverslips, and these were dried at 40°C; use of a warm temperature to facilitate drying resulted in a much more uniform distribution of purple membrane over the area of the sample. The mylar films were then taken off the glass coverslips and pairs were laid one on top of the other, face-to-face, so that the thin films of purple membrane were sandwiched between two mylar sheets. The final specimen prepared in this way consisted of a purple disk, slightly larger than 1 cm in diameter, with an optical density at 568 nm between 0.5 and 0.7.

Characterization of Optical Spectra

Optical spectra were obtained with thin films on mylar by clamping the films between two thin brass plates containing 5 × 5-mm square holes. The brass-plate holder was placed inside a specially constructed Pyrex cuvette, which itself could be placed into a specially fabricated Pyrex spectrophotometer dewar, the shape of which was designed to be suitable for fitting into the specimen chamber of the spectrophotometer. The

bottom of the curvette had five holes, each ~2 mm in diameter, which permitted cold nitrogen gas to rise up through the cuvette, thereby keeping the brass holder and the mylar film at a temperature measured to be between −90° and −100°C. Spectra of samples in the bR_{568} state were measured using the same apparatus at room temperature.

Samples of purple membrane on thin mylar films were converted to the M state by two different methods. In the first procedure the mylar films were held for one minute in front of the intense light from a 500-watt projection lamp, filtered by color glass (OG515; Barr and Stroud), which has a complete cutoff below ~525 nm. The films were then pulled out of the light and plunged into liquid nitrogen as quickly as possible. Such films were mounted into the brass-plate holder under liquid nitrogen, which was then transferred quickly into the precooled cuvette of the spectrophotometer dewar. In the second procedure the mylar films were mounted into the brass holder, which was then placed into the spectrophotometer dewar. The specimen chamber of the dewar itself was illuminated by the 500-watt projector. The thin film sample was thus slowly cooled by the gas from the boiling nitrogen, under continuous illumination. When this method was used, the level of light intensity and the specimen cooling rate (adjusted by use of an immersion heater in the bottom of the dewar to vary the rate of boil-off of nitrogen gas) had to be balanced empirically to prepare samples successfully in the M state.

X-ray Diffraction Patterns

X-ray diffraction patterns of specimens in the M state were obtained by stacking together 10 to 12 of the thin film samples, each of which had been individually converted to the M state and stored in liquid nitrogen. The stacked mylar films were clamped between two rings of brass under liquid nitrogen. Thin aluminum foil windows at the top and bottom of the stack served as convective and radiative heat shields. The clamped brass holder itself was then transferred from liquid nitrogen to a precooled specimen stage in an evacuated x-ray camera fitted with a rotating anode and toroidal focusing optics. The stage itself was cooled by a continuous flow of cold nitrogen gas passing through a copper tubing heat exchanger, soldered to a thermally insulated central piece of the stage. The temperature of the mylar films remained below −90°C during the course of the x-ray exposure, which was normally 4 h.

Electron Diffraction Measurements

Electron diffraction patterns were recorded from large, fused membrane sheets as described by Baldwin and Henderson (1984). Film densitometry and data processing also followed the procedures described previously (Baldwin and Henderson, 1984). All diffraction data were collected at low temperature (−120°C), using the gas-cooled cold stage for the electron microscope (model EM400; Philips Electron Instruments Inc., Mahwah, NJ). The decrease in the rate of radiation damage under these conditions (Hayward and Glaeser, 1979) made it possible to record diffraction patterns from smaller areas of membrane, thereby increasing the likelihood that the diffraction patterns would exhibit little or no twinning. Complete sets of electron diffraction data were collected under identical conditions for samples in the bR_{568} state as well as the M_{412} state to minimize systematic errors that might otherwise have existed due to factors such as the low specimen temperature or other details of specimen preparation and data collection.

Specimen grids used for collecting the electron diffraction data were prepared immediately before use by applying a 2-μl droplet of fused membranes, in detergent solution (Baldwin and Henderson, 1984), to hydrophobic carbon films on 400 mesh copper grids. After waiting 1 to 3 min the excess membranes and solution were washed off with two successive 50-μl drops of 1% glucose containing 0.02% sodium azide. The excess glucose solution was then drained off to complete dryness by touching the back side of the EM grid with the cut edge of filter paper (No. 1; Whatman Inc., Clifton, NJ). All specimens were first prepared and mounted under normal conditions of ambient lighting. They were then subjected as described below to a further period of incubation either

in the dark or under illumination, to give specimens that we assume are in a similar state to the normal bR_{568} and M_{412}, respectively.

Specimens used for data collection on what we believe is the bR_{568} state were first held in complete darkness for 1 to 2 min. These specimens were then inserted into the microscope column and cooled to below −120°C before turning on the room lights. These precautions were taken because it is known that the photocycle of dried purple membrane is much slower than that of native, hydrated membranes (Lazarev and Terpugov, 1980), and we wished to ensure that all molecules of bacteriorhodopsin had advanced through the photocycle, back to the bR_{568} state, before the specimen was evacuated and cooled.

Specimens used for data collection in what we believe is the M_{412} state were prepared by first holding the specimen grid in the intense light beam from the 500-watt projection lamp, filtered by the color glass. After waiting ∼1 min, the sample was cooled by turning on the cold gas flow for the cold stage. The sample and cold-holder were protected at this point against condensation of water from the atmosphere by a continuous flow of dry N_2 gas through a shroud of thin walled (flexible) clear plastic tubing. When the specimen temperature was below −90°C (∼2–3 min after starting the cold gas flow), the sample holder was taken out of the intense light, the protective copper cold shroud of the cold stage was moved into the closed position, and the specimen rod was inserted into the electron microscope. The specimen was then held in the airlock for at least 2 min under continuous pumping to remove water that condenses onto the exposed cold surfaces of the shroud during transfer from the dry nitrogen purge to the airlock. In spite of these precautions, the EM grid normally had a fairly thick film of water condensed onto the specimen, and it was necessary to warm the specimen to −90°C to remove condensed water by sublimation. The specimen was then cooled again to −120°C for data collection.

RESULTS

Visible Absorption Spectra

Bleaching of the purple samples to a light yellow color occurred when the thin-film samples were converted to the M-intermediate state by either of the procedures described above, and rapid recovery of the purple color occurred when the thin films were warmed again. Measurement of the actual spectra, as shown in Fig. 1, confirmed that >90% of the bR molecules were trapped in the M state in specimens prepared by either procedure. The spectra of samples recorded at room temperature showed that bR is

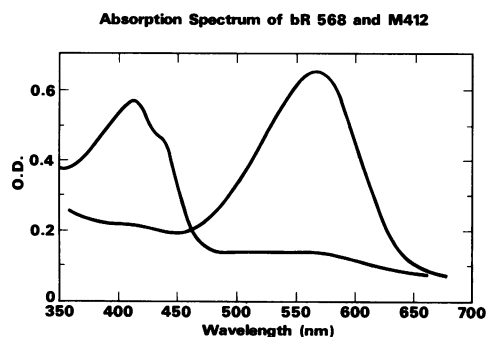**Absorption Spectrum of bR 568 and M412**

FIGURE 1 Absorption spectra obtained from a thin-film sample of glucose-embedded purple membrane (a) at room temperature and (b) at low temperature, after conversion to the M state as described in the text. Both spectra were recorded with the sample held in a pyrex spectrophotometer dewar. The baseline for both curves is arbitrary due to the absence of an equivalent blank specimen in the reference beam.

normally in the light-adapted state in the glucose-embedded samples. The two types of spectra shown in Fig. 1 have been redrawn to eliminate small ripples with an amplitude of 0.01–0.02 OD units, which we attribute to interference effects (Newton's rings) between the two mylar films, and also to place the spectra on the same baseline. The baseline is necessarily arbitrary in these spectra as they were recorded without an equivalent blank sample in the reference beam.

X-ray Diffraction

X-ray diffraction patterns recorded from the thin film samples show that there normally is no observable difference between samples in the M state and those in the bR_{568} state in either the sharpness of the diffraction rings or the resolution to which the rings can be recorded. In one M-state specimen, however, which was prepared by the slow cooling method, there was an appreciable broadening of the diffraction rings, suggesting that a significant reduction in order had occurred. Although several attempts were made to find conditions of cooling rate and light intensity that could reproduce this effect, we were unable to prepare M-state samples again whose x-ray patterns were significantly different from those of samples that were in the light adapted, bR_{568} state. Fig. 2 shows a comparison of representative x-ray patterns obtained for samples in the M state and the light-adapted, bR_{568} state. Also shown here is the photograph of the one sample in the M state that exhibited significant broadening of the diffraction rings. Visible absorption spectra were also recorded for thin films after removal from the x-ray diffraction cold stage, and these spectra confirmed that the specimens were still >90% in the M state after completion of the 4-h x-ray exposure.

Electron Diffraction

Electron diffraction patterns obtained from samples in the M state show no differences that are obvious, on visual inspection, relative to patterns recorded for light-adapted specimens. There is no apparent change in the degree of crystalline order, and this point is confirmed by a quantitative comparison of temperature factors obtained during scaling of films after densitometry. The lattice parameter was measured relative to an internal standard, using the 3.66 Å diffraction ring of cubic ice that was intentionally condensed onto the surface of the specimen. The measured value in both cases was 62.4 Å, within experimental error (0.1 Å).

Difference amplitudes (ΔF values) were calculated for common points for the two independent data sets. The first set of ΔF values was derived from diffraction patterns of nominally untilted specimens, and this data set consisted of six films of the bR_{568} specimen and six films of the M_{412} specimen. The second set of ΔF values was derived from diffraction patterns of specimens tilted nominally by 20°,
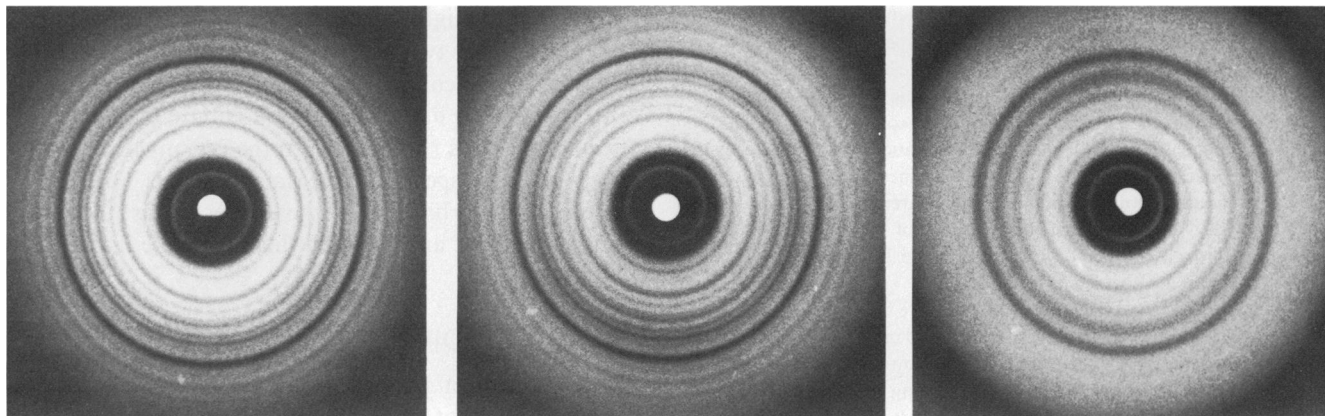
FIGURE 2 X-ray diffraction patterns recorded for thin films of purple membrane embedded in glucose. Typical examples of samples in (a) the bR_{568} state and (b) the M_{412} state are shown, along with (c) an atypical, partially disordered pattern recorded for one sample in the M_{412} state.

and that data set consisted of 35 films of the bR_{568} specimen and 37 films of the M_{412} specimen. In both cases smooth curves were fitted to the experimental values of intensity when plotted on reciprocal lattice lines (hkZ*), as described by Baldwin and Henderson (1984). Two examples of such curves are shown in Fig. 3. The intensities corresponding to the values of each curve at equivalent reciprocal lattice points were then used to calculate

$$\Delta F = F_{412} - F_{568}, \quad (1)$$

where F_{412} is the structure factor amplitude for samples in the M_{412} state and F_{568} is the structure factor amplitude for samples in the bR_{568} state.

The degree of similarity between these two independent data sets was judged by computing the sample correlation coefficient (Hoel, 1971)

$$C = \frac{\Sigma\Delta F_1\Delta F_2 - \dfrac{\Sigma\Delta F_1\Sigma\Delta F_2}{n}}{\left\{\Sigma(\Delta F_1)^2 - \dfrac{(\Sigma\Delta F_1)^2}{n}\right\}^{1/2}\left\{\Sigma(\Delta F_2)^2 - \dfrac{(\Sigma\Delta F_2)^2}{n}\right\}^{1/2}}, \quad (2)$$

where ΔF_1 and ΔF_2 are the difference amplitudes of the first and second data sets, respectively; the summation is taken over sets of reflections lying within successive annular zones of reciprocal space; and n is the number of reflections in the zone. Table I shows each of the resolution zones for which the correlation coefficient was calculated. As can be seen in the table, there is very little similarity in ΔF values at a resolution below ~5.0 Å, but there is a significant correlation in the values of ΔF for the two data sets at high resolution.

The observed values of ΔF_1 and ΔF_2, together with the correlation coefficient, can be used to obtain a statistical estimate of the magnitude of the structural change occurring in the M intermediate. The modulus of the true ΔF, as distinct from the noise in the measurement, is estimated

from

$$|\overline{\Delta F}| = (c|\overline{\Delta F_1}||\overline{\Delta F_2}|)^{1/2}, \quad (3)$$

where $|\overline{\Delta F_1}|$ and $|\overline{\Delta F_2}|$ are the mean values, within annular resolution zones, of the modulus of ΔF for the two indepen-
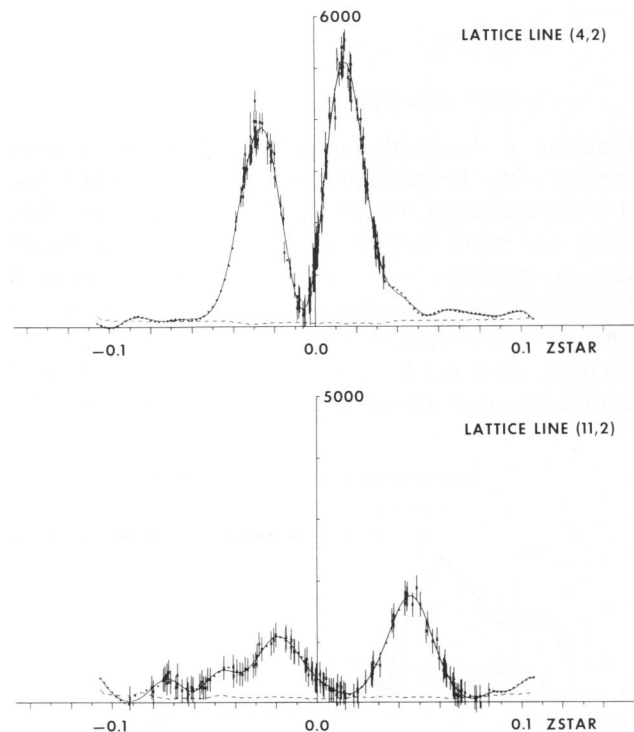

FIGURE 3 Representative examples of the merged electron diffraction data obtained from samples in the M_{412} state that were titled to an angle of 20°. The dashed curve near the baseline is the root mean square error in the fitted curve. The small plus marks seen along the curve that extends beyond the data points, and occasionally between data points, represent tie points derived from the data set of Balwin and Henderson (1984); these tie points were used to constrain the fitted curve at points where the data is sparse and at the edges of the collected data.

TABLE I

STATISTICAL EVALUATION OF THE DIFFERENCE IN
DIFFRACTION AMPLITUDES FOR bR_{568} AND M_{412}, AND
THE IMPLIED STRUCTURAL DIFFERENCE

Resolution zone Å	Number of unique reflections	Correlation coefficient	$|\overline{\Delta F}|$*	$|\overline{F}|$‡	m§
15–6.7	15	0.09	158	12,095	0.4
6.7–5.0	34	0.10	108	6,237	0.7
5.0–4.2	90	0.30	218	4,184	6.2
4.2–3.7	96	0.29	204	4,336	5.1
3.7–3.3	32	0.34	200	3,492	7.5

*Estimated mean value of the signal based on observed values of ΔF and the correlation coefficient. See Eq. 3.
‡Mean value of the structure factor amplitude for each resolution zone.
§Estimated number of atoms that would have to move to produce the observed $|\overline{\Delta F}|/|\overline{F}|$.

dent data sets; c is the correlation coefficient. The estimated values of the true ΔF derived in this way are shown in Table I. The number of atoms moving by a distance comparable to the resolution of a given annular zone is then estimated from

$$m = N\left(\frac{|\overline{\Delta F}|}{|\overline{F}|}\right)^2, \tag{4}$$

where N is the total number of atoms in the structure, excluding hydrogen, and $|\overline{F}|$ is the mean value of the modulus of the structure factor within the annular resolution zone. Eq. 4 is obtained from the formula of Crick and Magdoff (1956), which is normally used to estimate mean intensity changes in isomorphous heavy atom derivatives. In our case the number of extra atoms is set equal to twice the number of nonhydrogen atoms that have moved. The factor of two accounts for the addition of atoms at the new sites plus the removal of atoms from previously occupied sites. The value of N used in Eq. 4 was estimated to be 2,300, including 1,913 atoms from bacteriorhodopsin and ~400 atoms due to lipid molecules within the unit cell. The estimated number of atoms that move by a given amount is shown in Table I. Effectively no atoms move by large distances (low resolution), but there is good evidence that ~5 to 7 atoms move by distances in the range of 3–5 Å.

Difference Fourier Map

A difference Fourier map was calculated using the equatorial, (hkO) difference amplitudes obtained here and the corresponding high resolution phases published by Henderson et al. (1986). The difference map, shown in Fig. 4, contains several peaks of positive and negative density, two or more contour levels in height, within the molecular envelope of the protein. A prominent positive-negative pair of density peaks is also seen in the lipid-filled space at the center of the protein trimer, but no significant density differences are seen in the region of lipid that surrounds the
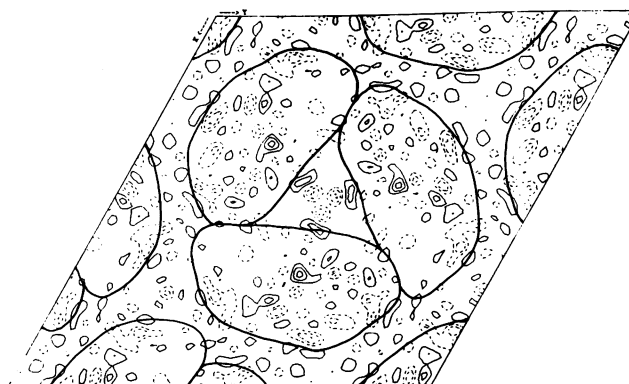

FIGURE 4 The two-dimensional difference Fourier map, which shows changes in the projected density upon formation of the M-state structural intermediate.

protein trimers. As a point of reference, a single contour-interval in Fig. 4 corresponds to a density difference that is only two per cent of the peak density of a typical helix in the native density map. The largest peak heights seen in the map therefore represent density changes that are only a small fraction of the total projected density. Furthermore, the widths of the largest difference peaks are only in the range of 3–4 Å. The features seen in the difference map are therefore fully consistent with the conclusions that were drawn above, that the structural changes involved in formation of the M intermediate are limited to high resolution features, and involve the movement of only a few nonhydrogen atoms.

DISCUSSION

We have so far made only statistical statements about the structural changes that occur in the formation of the M intermediate state of bR. More specific details of these structural changes could be obtained from a difference Fourier map, if high resolution phases were available in three dimensions. The high resolution phases available at this time are limited, however, to a single two-dimensional projection, and consequently the observed peaks in the difference map cannot yet be interpreted in molecular detail. The magnitudes of the difference amplitudes that we have already observed in the resolution zone from 5.0 to 3.3 Å are large enough, however, to expect that interpretable difference peaks should be seen in a three-dimensional, high resolution difference map, when the high resolution phases do become available.

The statistical estimates of structural change, which are presented in Table I, put substantial constraints on models that can be proposed for the molecular mechanism of proton pumping by bR. The total change in structure that has been observed is equivalent to the movement of a few nonhydrogen atoms by distances of <5 Å. Part of this change in structure is probably associated with the movement of atoms in the vicinity of the C13–C14 double bond

of the retinal group, during *trans-cis* isomerization. High resolution, solid state NMR spectroscopy indicates that this isomerization is accomplished with a complex set of bond rotations that leave most atoms of the retinal group in approximately their original positions (Harbison et al., 1984), and thus it is unlikely that isomerization of the retinal group is the only change that contributes to the observed intensity differences. The remaining structural change may therefore involve the additional movement of only a few amino acid side chains. It is important to qualify this discussion, however, with the observation that the electron diffraction data analyzed here would be insensitive to additional movements in a direction perpendicular to the plane of the membrane.

Some of the published spectroscopic and other biophysical measurements relating to the M intermediate are most easily interpreted in terms of rather large conformational changes. Among the evidence that suggests a substantial change in conformation, one can include changes in the UV absorption spectra and the fluorescence spectra of aromatic amino acid side chains, changes in the net electrostatic dipole moment of the protein, transient changes in the photo-induced linear dichroism, apparent disorder observed in time-resolved x-ray diffraction patterns from oriented stacks of membranes, effects measured in the circular dichrosim spectra at both visible and far UV wavelengths, and the influence of environmental perturbations on photocycle kinetics. Each of these areas is addressed more fully in the following paragraphs.

The peak extinction coefficient in the near UV is estimated to decrease by $\sim 5,000 \text{ cm}^{-1} \text{ mol}^{-1}$ during formation of the M intermediate (Becher et al., 1978). Both a change in the "solvent perturbation effect" (Donovan, 1969) or a change in the stacking geometry of aromatic rings could account for the observed far UV hypochromism. In addition, Rafferty (1979) has concluded that a change in the UV absorption spectrum of the retinal group in the M state makes "a significant probably predominant contribution to the difference spectrum between 250 nm and 300 nm." Becher et al. (1978) suggested that about half of the tyrosine and tryptophan side chains would have to move from the hydrophobic interior of the protein to the aqueous medium, if the solvent perturbation effect were to account for the measured decrease in extinction coefficient. Movement of half of the tyrosine and tryptophan residues from a nonpolar environment to a polar environment is more suggestive of massive denaturation than of a subtle shift in conformation, and thus a model involving relatively small displacements in the stacking geometry of these side chains seems more compatible with the new data from electron diffraction experiments. It should be noted, however, that theoretical assignments of the primary amino acid sequence to seven runs of α-helix, such as the model proposed by Engelman et al. (1980), place more than half of the tyrosine and tryptophan residues near to

the surface of the membrane. Thus, it would indeed be possible for these residues to flip between hydrophobic and hydrophilic environments with little displacement in the projected positions of their side chains. That a few aromatic residues—but only a few—do move from a nonpolar environment to a polar environment is supported by measurements of wavelength shifts and intensity changes in the intrinsic fluorescence of the protein and by measurements of fluorescence quenching with cesium ions (Bogolmolni et al., 1978).

A major asymmetry in surface charge (Ehrenberg and Berezin, 1984; Renthal and Cha, 1984) makes it possible to orient purple membrane sheets by the application of low-frequency electric fields (Kimura et al., 1984). Measurement of the degree of orientation achieved at a given field strength makes it possible to estimate the transmembrane dipole moment per molecule of bR and thus the net asymmetry in surface charge. Application of these techniques to bR in the M state shows that the asymmetry in surface charge is reduced to approximately two thirds of its initial value (Kimura et al., 1984). It is not known whether this change represents the neutralization of charges on the cytoplasmic surface or the ionic dissociation of charged residues on the extracellular surface. Either way, the electrostatic measurements suggest a substantial degree of conformational change involving surface groups. Without a detailed solution of the structure of the protein, however, it is difficult to know whether the changes in surface charge can be achieved as a result of very slight structural changes, as suggested by our electron diffraction data.

Complex rotational displacements of individual bR monomers in the M state, along with the rotation of noncycling, neighboring molecules (induced by formation of molecules in the M state), have been proposed to account for the transient responses of linear dichroism that are observed after a short pulse of actinic light (Ahl and Cone, 1984). These molecular rotations are highly temperature-sensitive, and it appears that they can also be prevented by immobilization of membrane sheets in polyacrylimide or agarose gels. At first sight it would seem that molecular rotations by $20°$ to $30°$ could only occur due to substantial changes in the lattice bonding forces, thereby implying quite large changes in protein conformation. An alternative possibility, however, that has been suggested by Frankel and Forsyth (1985), is that the molecular rotations are a response to changes in the long-range electrostatic forces, which follow from the previously mentioned changes in the number and position of surface charges. The rotation of intact trimers in response to changes in electrostatic forces is particularly easy to visualize, since the trimers are completely surrounded by a boundary layer of lipid, and there are no direct protein-protein contacts between trimers (Glaeser et al., 1985). Rotational slippage between the trimers and the intervening lipid molecules could thus occur without requiring a noticeable change in

918

protein structure other than the already known changes in surface charge distribution.

Time-resolved x-ray diffraction patterns of bR in the M state have indicated that there often is a substantial change in both the short-range and long-range order of the crystalline lattice immediately after conversion of the membranes to the M state (Frankel and Forsyth, 1985). A noticeable decrease in long-range order was also observed in one specimen that we prepared during one of our control x-ray experiments, before collecting electron diffraction data (c.f., Fig. 2). It is possible that the disorder observed in certain x-ray diffraction experiments results from transient molecular rotations of the type observed in the linear dichroism measurements of Ahl and Cone (1984). The fact that these molecular rotations have a complex dependence upon temperature and can apparently be inhibited by the immobilizing effect of the surrounding matrix may explain why we were unable to discover conditions under which the formation of disordered specimens could be reproduced. Frankel and Forsyth (1985) also reported that the disorder apparent in time-resolved x-ray photographs varies from one experiment to the next.

In any case, we observed no significant difference in the degree of order of specimens prepared for electron diffraction experiments. This fact could possibly be due to the immobilizing effect of the surrounding glucose embedment in such specimens, similar to the effect of acrylimide or agarose gels reported by Ahl and Cone (1984). Alternatively, the rotational disorder might have been removed by a process of annealing when the specimens were converted fully to the M state and, unlike the situation in time-resolved studies, they were held there for a long time, before cooling the sample to $-100°C$.

Complete disordering of the crystalline lattice, involving even the loss of threefold rotational symmetry between bR monomers, is suggested by the loss of exciton-coupled splitting of the visible CD band in the M state (Draheim and Cassim, 1985), in samples prepared in high salt at high pH, in the presence of high amounts of glycerol. It is intriguing to speculate that differences in the electrostatic forces under these conditions might cause substantial disorder, whereas glucose-embedded samples (proven to be in the M state as determined by their visible absorption spectrum at the end of the experiments) can be prepared that show no measurable loss of crystalline order in their x-ray photographs.

The kinetics of the photocycle and particularly the formation and decay of the M intermediate, show a dependence on environment conditions such as pH (Kalisky et al., 1981; Fukumoto et al., 1984), solvent viscosity (Beece et al., 1981), degree of hydration (Lazarev and Terpugov, 1980; Korenstein and Hess, 1977), and hydrostatic pressure (Tsuda et al., 1983). While each one of these effects argues for the existence of a change in protein conformation, they provide no direct indication of the

magnitude of the conformational change, and none of these observed effects on the photocycle kinetics is inconsistent with the rather small changes inferred from the electron diffraction data.

Far UV circular dichroism spectra of oriented specimens have been interpreted to show a substantial change in the tilt angle of the transmembrane helices of bR in the M state (Draheim and Cassim, 1985). This interpretation is in sharp conflict with the evidence presented by our electron diffraction data. The tilting of a single helix by as much as 10° would produce a lateral shift of all amino acid residues at one end of the helix by 5 Å or more relative to those at the other end of the helix. Structural changes of this magnitude would have produced much larger intensity changes in the diffraction patterns than those we actually observed.

Time-resolved measurements of volume changes during the photocyle have indicated that the metastable state that is formed on a time-scale similar to that of the M intermediate is associated with an enthalpy change of -36 kcal/mol (Ort and Parson, 1979). Such an enthalpy change would require, in turn, a decrease in entropy of at least 125 cal/mol-deg. A decrease in entropy of the protein by such a large amount — comparable to the entropy increase cited by Ort and Parson as accompanying the unfolding of lysozyme — is unlikely to be due to an increase in order of the crystalline lattice, since the bR_{568} state is already quite well ordered. Creation of dissociated ion pairs can decrease the entropy of an aqueous system by 15–30 cal/mol-deg (Sturtevant, 1977). Thus the observed change in the surface charge of the M intermediate might be a major factor contributing to the measurements of Ort and Parson. The estimates of enthalpy and entropy changes themselves are uncertain, however, since they depend upon the assumption that volume changes for processes such as the formation of ionized species are independent of temperature. As noted by Arata and Parson (1981), this assumption may not be valid, and therefore there may be substantial errors in the thermodynamic estimates.

There is one important technical limitation in our use of electron diffraction data to study structural intermediates. It is impractical to determine by spectroscopic means whether single glucose-embedded membranes, prepared on carbon-coated grids, have actually been converted to the desired structural intermediate. We have therefore had to assume that the conditions that work for thick films of glucose-embedded membranes will also be successful for the single membranes mounted on carbon films. The validity of our assumption will ultimately be testable when three-dimensional high resolution phases become available. Specific structural changes should then be identifiable, through the use of electron diffraction intensities to compute a high-resolution difference map. At that point it will be possible to tell whether precisely determined structural changes occur in these specimens that account fully

for the spectroscopic data that has already been obtained with the M intermediate.

REFERENCES

Ahl, P. L., and R. A. Cone. 1984. Light activates rotations of bacteriorhodopsin in the purple membrane. *Biophys. J.* 45:1039–1049.

Arata, H., and W. W. Parson. 1981. Delayed fluorescence from *Rhodopseudomonas sphaeroides* reaction centers. Enthalpy and free energy changes accompanying electron transfer from p-870 to quinones. *Biochim. Biophys. Acta.* 638:201–209.

Baldwin, J., and R. Henderson. 1984. Measurement and evaluation of electron diffraction patterns from two-dimensional crystals. *Ultramicroscopy.* 14:319–336.

Becher, B., F. Tokunaga, and T. G. Ebrey. 1978. Ultraviolet and visible absorption spectra of the purple membrane protein and the photocycle intermediates. *Biochemistry.* 17:2293–2300.

Beece, D., S. F. Bowne, J. Czege, L. Eisenstein, H. Frauenfelder, D. Good, M. C. Marden, J. Marque, P. Ormos, L. Reinisch, and K. T. Yue. 1981. The effect of viscosity on the photocycle of bacteriorhodopsin. *Photochem. Photobiol.* 33:517–522.

Bogomolni, R. A., L. Stubbs, and J. Lanyi. 1978. Illumination-dependent changes in the intrinsic fluorescence of bacteriorhodopsin. *Biochemistry.* 17:1037–1041.

Braiman, M., and R. Mathies. 1980. Resonance Raman evidence for an all-*trans* to 13-*cis* isomerization in the proton-pumping cycle of bacteriorhodospin. *Biochemistry.* 19:5421–5428.

Crick, F. H. C., and B. S. Magdoff. 1965. The theory of the method of isomorphous replacement for protein crystals. I. *Acta Crystallogr. Sect. B Struct. Crystallogr. Cryst. Chem.* 9:901–908.

Donovan, J. W. 1969. Ultraviolet absorption. *In* Physical Principles and Techniques of Protein Chemistry. S. J. Leach, editor. Academic Press, Inc., New York. 101–170.

Draheim, J. E., and J. Y. Cassim. 1985. Large scale global structural changes of the purple membrane during the photocyle. *Biophys. J.* 47:497–508.

Engelman, D. M., R. Henderson, A. D. McLachlan, and B. A. Wallace. 1980. Path of the polypeptide in bacteriorhodopsin. *Proc. Natl. Acad. Sci. USA.* 77:2023–2027.

Ehrenberg, B., and Y. Berezin. 1984. Surface potential on purple membranes and its sidedness studied by a resonance Raman dye probe. *Biophys. J.* 45:663–670.

Frankel, R. D., and J. M. Forsyth. 1985. Time-resolved x-ray diffraction study of photo-stimulated purple membrane. *Biophys. J.* 47:387–393.

Fukumoto, J. M., J. H. Hanamoto, and M. A. El-Sayed. 1984. On the tyrosinate involvement in the Schiff base deprotonation in the proton pump cycle of bacteriorhodopsin. *Photochem. Photobiol.* 39:75–79.

Glaeser, R. M., J. S. Jubb, and R. Henderson. 1985. Structural compari-

son of native and deoxycholate-treated purple membrane. *Biophys. J.* 48:775–780.

Harbison, G. S., S. O. Smith, J. A. Pardoen, C. Winkel, J. Lugtenburg, J. Herzfeld, R. Mathies, and R. G. Griffin. 1984. Dark-adapted bacteriorhodopsin contains 13-*cis*, 15-*syn*, and all-*trans*, 15-*anti* retinal Schiff bases. *Proc. Natl. Acad. Sci. USA.* 81:1706–1709.

Hayward, S. B., and R. M. Glaeser. 1979. Radiation damage of purple membrane at low temperature. *Ultramicroscopy.* 4:201–210.

Henderson, R., J. M. Baldwin, K. H. Downing, J. Lepault, and F. Zemlin. 1986. Structure of purple membrane from *Halobacterium halobium*: recording, measurement and evaluation of electron micrographs at 3.5-Å resolution. *Ultramicroscopy.* 19:147–178.

Hoel, P. G. 1971. Introduction to Mathematical Statistics. Fourth Ed. John Wiley & Sons, New York. 164.

Kalisky, O., M. Ottolenghi, B. Honig, and R. Korenstein. 1981. Environmental effects on formation and photoreaction of the M_{412} photoproduct of bacteriorhodopsin: implications for the mechanism of proton pumping. *Biochemistry.* 20:649–655.

Kimura, Y., M. Fujiwara, and A. Ikegami. 1984. Anisotropic electric properties of purple membrane and their change during the photoreaction cycle. *Biophys. J.* 45:615–625.

Korenstein, R., and B. Hess. 1977. Hydration effects on the photocycle of bacteriorhodopsin in thin layers of purple membrane. *Nature (Lond.).* 270:184–186.

Lazarev, Y. A., and E. L. Terpugov. 1980. Effect of water on the structure of bacteriorhodopsin and photochemical processes in purple membrane. *Biochim. Biophys. Acta.* 590:324–338.

Lewis, A., J. Spoonhower, R. A. Bogomolni, R. H. Lozier, and W. Stoeckenius. 1974. Tunable laser resonance Raman spectroscopy of bacteriorhodopsin. *Proc. Natl. Acad. Sci. USA.* 71:4462–4466.

Lozier, R. H., and W. Niederberger. 1977. The photochemical cycle of bacteriorhodopsin. *Fed. Proc.* 36:1805–1809.

Oesterhelt, D., and W. Stoeckenius. 1971. Rhodopsin-like protein from the purple membrane of *Halobacterium halobium. Nature New Biol.* 233:149–152.

Oesterhelt, D., and W. Stoeckenius. 1973. Functions of a new photoreceptor membrane. *Proc. Natl. Acad. Sci. USA.* 70:2853–2857.

Ort, D. R., and W. W. Parson. 1979. Enthalpy changes during the photochemical cycle of bacteriorhodopsin. *Biophys. J.* 25:355–364.

Rafferty, C. N. 1979. Light-induced perturbation of aromatic residues in bovine rhodopsin and bacteriorhodopsin. *Photochem. Photobiol.* 29:109–120.

Renthal, R., and C.-H. Cha. 1984. Charge asymmetry of the purple membrane measured by uranyl quenching of dansyl fluorescence. *Biophys. J.* 45:1001–1006.

Rosenbach, V., R. Goldberg, C. Gilon, and M. Ottolenghi. 1982. On the role of tyrosine in the photocycle of bacteriorhodopsin. *Photochem. Photobiol.* 36:197–201.

Rothschild, K. J., M. Zagaeski, and W. A. Cantore. 1981. Conformation changes of bacteriorhodopsin detected by Fourier transform infrared difference spectroscopy. *Biochem. Biophys. Res. Commun.* 103:483–489.

Siebert, F., W. Mantele, and W. Kreutz. 1982. Evidence for the protonation of two internal carboxylic groups during the photocycle of bacteriorhodopsin. *FEBS (Fed. Eur. Biochem. Soc.) Lett.* . 141:82–87.

Sturtevant, J. M. 1977. Heat capacity and entropy changes in processes involving proteins. *Proc. Natl. Acad. Sci. USA.* 74:2236–2240.

Tsuda, M., R. Govindjee, and T. G. Ebrey. 1983. Effects of pressure and temperature on the M_{412} intermediate of the bacteriorhodopsin photocycle. *Biophys. J. A* 44:249–254.